BULLETIN OF THE POLISH ACADEMY OF SCIENCES
TECHNICAL SCIENCES, Vol. 66, No. 5, 2018
DOI: 10.24425/125336

Current harmonic controller in multiple reference frames for series active power filter integrated with 18-pulse diode rectifier

W. ŚLESZYŃSKI[1]*, A. CICHOWSKI[1], and P. MYSIAK[2]

[1]Faculty of Electrical and Control Engineering, Gdańsk University of Technology, 11/12 Narutowicza St., 80-233 Gdańsk, Poland
[2]Faculty of Electrical Engineering, Gdynia Maritime University, 81-87 Morska St., 81-225 Gdynia, Poland

Abstract. The paper presents the control system and selected results of experimental tests of the AC/DC power converter consisting of an 18-pulse diode rectifier based on coupled reactors and a serial active power filter. Proportional integral controllers with decoupling components are implemented in multiple reference frames for selective line current harmonic suppression. The regulator is provided with a backtracking anti-windup mechanism of sorts in which a signal proportional to the saturated control reference is subtracted from the error signal in each reference frame. The fundamental harmonic filter based on the DFT algorithm with phase correction is used for grid synchronization and current harmonic detection. Three configurations of the 15 kVA converter were tested experimentally and then compared: the 18-pulse diode rectifier with and without an additional grid reactor, and the rectifier integrated with an active power filter. The applied control method of active filter significantly reduces harmonic distortion and unbalance of the grid current, which is particularly advantageous under non-ideal supply voltage and low loads conditions.

Key words: series active power filters, multi-pulse converters, diode rectifier, power conditioning.

1. Introduction

Three-phase diode rectifiers with capacitive filters are frequently used in the industry because of their low cost, high reliability and low-level emission of disturbances. Unfortunately, their input currents are highly distorted. Yet it is possible to reduce undesired harmonics in the supply current by using a multi-pulse diode rectifier [1]. Reference [2] presents an 18-pulse diode rectifier with coupled reactors, which makes it possible to reduce undesired harmonics in the supply current. Its advantage, in comparison to other 18-pulse converters with transformers or autotransformers, is the distinctly smaller limiting power of the electromagnetic elements required, which obviously results in smaller dimensions and weight of the entire rectifying device. Unfortunately, this special rectifier manifests small resistance to voltage disturbances in the supply network [2]. The solution to the abovementioned problem seems to take the form of a small-rated series active power filter (S-APF), which further improves the power quality [3–7].

Several current control methods of an S-APF integrated with multi-pulse rectifiers can be found in the literature [4–7]. In early analog solutions [4, 5], the fundamental harmonic component was filtered out from the supply current and the resulting control error was amplified. However, in digital control, due to inherent delays in the S-APF control system, this method proved to be useless in practice [6]. Instead, the DFT-based control algorithm was proposed [6], in which only the dominant harmonics of the supply current are isolated and suppressed. However, the authors did not provide design guidelines for the controller parameters. Digital control of an S-APF as a current source was proposed in [7]. A hysteresis controller was used to shape the phase currents on the inverter side of the injection transformer.

This paper presents the control system of the series active power filter for suppression of input current harmonics in the 18-pulse rectifier with an output capacitive filter. The current harmonic controller consists of multiple regulators operating in parallel in the reference frames rotating synchronously with the angular frequencies of dominant harmonics of the current. The performance of the integrated system was compared with a stand-alone 18-pulse diode rectifier with and without an additional grid reactor.

2. Integrated supply system

A simplified block diagram of the proposed AC/DC supply system is presented in Fig. 1. It is composed of an 18-pulse rectifier and a series active power filter. The three-phase supply is represented by the source voltage e_S and the line inductance L_S. 18-pulse operation of the rectifier is obtained using a current dividing transformer (CDT) for preliminary current division, and a set of coupled three-phase reactors (CTR) [2]. These magnetic elements form three systems of three-phase voltages, shifted by 20° with respect to each other. The 6-pulse rectifiers are connected to the outputs of the coupled three-phase reactors. Such a structure of the AC/DC converter provides opportunities for reduction of undesired higher harmonics in the grid current, mainly of an order of 5, 7, 11 and 13.

*e-mail: wojciech.sleszynski@pg.edu.pl

Manuscript submitted 2018-03-07, revised 2018-06-12 and 2018-07-23, initially accepted for publication 2018-07-30, published in October 2018.

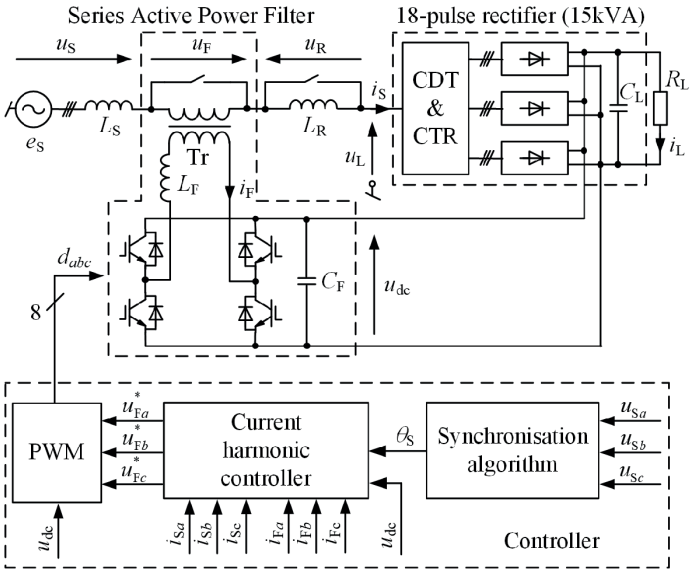

Fig. 1. Schematic diagram of the AC/DC supply system based on 18-pulse rectifier and series active power filter

The series active power filter comprises three fully single-phase circuits consisting of a booster transformer (Tr) with voltage ratio 1:12, an optional filtering reactor L_F and an IGBTs voltage source inverter, the DC circuit of which is connected to the 18-pulse rectifier output. During start-up of the system and stand-alone operation of the rectifier, the S-APF is bypassed by a contactor. The control objectives are achieved with measurements of the supply voltages and currents, the phase currents of voltage source inverters (VSI) and the DC output voltage of the rectifier.

The proposed supply system has been designed as modular. The 18-pulse rectifier and the S-APF were built as two separate devices, which, when connected, form a single supply system. However, autonomous operation of the 18-pulse rectifier is also possible. The control algorithm was implemented on a TMS320C6713 signal processor combined with a Cyclone IV field programmable gate array.

3. S-APF control method

The main task of the serial active power filter in the proposed supply system is to block harmonic currents in the power supply at the smallest possible losses. For this reason, the fundamental component of the supply current is not adjusted. A simplified block diagram of the S-APF controller is shown at the bottom of Fig. 2. It consists mainly of the synchronization algorithm, the harmonic current controller and the pulse width modulation unit.

3.1. Fundamental component filter. The current harmonic controller applied in multiple reference frames (MRF) requires the instantaneous phase (θ_S) of the fundamental component of the supply voltage. The fundamental component filter is also used for calculating the harmonic current and then the control error (Fig. 2).

The control system presented herein makes use of the phase estimation method based on the Recursive Discrete Fourier Transform (RDFT) with phase offset correction. This method was originally elaborated in [8] for real-valued signals. It has been adopted here for analyzing the complex-valued signal obtained as a result of Clarke transformation of three phase signals ($x_{\alpha\beta} = x_\alpha + \mathrm{j}x_\beta$).

The periodic signal $x(t)$ with period T_1 is sampled with the constant sampling period T_s to produce the time sequence $x[k]$. The RDFT calculating the amplitude ($X_1[k]$) of the fundamental component of the signal can be written as:

$$X_1[k] = X_1[k-1] + \frac{1}{N}\left(x[k] - x[k-N]\right)e^{-\mathrm{j}\frac{2\pi}{N}k}. \qquad (1)$$

The RDFT time window $T_w = NT_s$ is assumed equal to the nominal period of the signal. Its fundamental component at instant k can be evaluated using Inverse DFT:

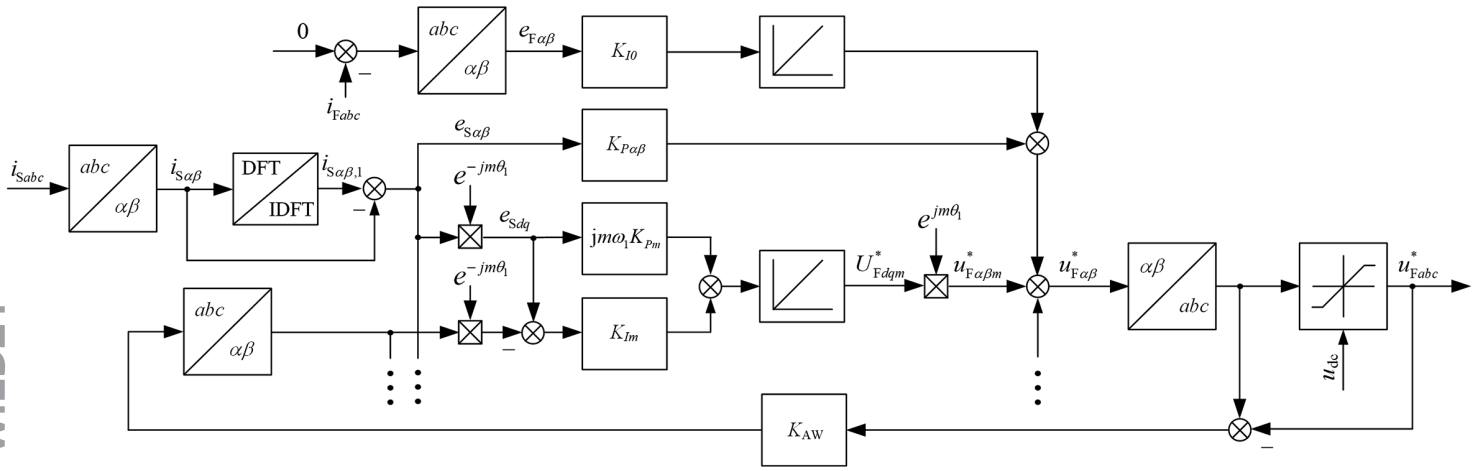

Fig. 2. Schematic diagram of current harmonic controller

$$x_1[k] = |X_1[k]|e^{j\varphi_1[k]}e^{j\frac{2\pi}{N}k} = |X_1[k]|e^{j\theta_1[k]}, \tag{2}$$

where θ_1 is the instantaneous phase and φ_1 is the RDFT phase calculation, given by:

$$\varphi_1[k] = \tan^{-1}\left(\frac{\mathrm{Im}\{X_1[k]\}}{\mathrm{Re}\{X_1[k]\}}\right), \tag{3}$$

When the RDFT time window T_w does not match the signal period T_1, it causes a phase shift between the measured signal $x[k]$ and the filtered fundamental component $x_1[k]$. Knowing the phase response of the fundamental component filter, it is possible to eliminate the phase error in $x_1[k]$ by adding an opposite phase shift into the inverse DFT calculation (2).

The transfer function of the RDFT/IDFT filter is given by the following:

$$\frac{X_1(z)}{X(z)} = \frac{1}{N}\frac{1-z^{-N}}{1-e^{j\frac{2\pi}{N}}z^{-1}}. \tag{4}$$

After substituting

$$z = e^{j2\pi\frac{f}{f_s}} = e^{j\frac{2\pi T_w}{NT_1}} \tag{5}$$

into (4) and some calculations, the frequency response of the filter can be expressed in a form allowing analysis of the impact of the DFT window mismatch on the signal period, i.e.:

$$H = \left[e^{j\frac{2\pi T_w}{NT_1}}\right] = \frac{\sin\left(\pi\left(\frac{T_w}{T_1}-1\right)\right)}{\sin\left(\frac{\pi}{N}\left(\frac{T_w}{T_1}-1\right)\right)}\frac{e^{-j\pi\left(\frac{N-1}{N}\right)\left(\frac{T_w}{T_1}-1\right)}}{N}. \tag{6}$$

The grid period T_1 is not known, therefore it is not possible to directly calculate the phase error based on the phase response of the filter. However, the phase correction can be estimated from current and previous values of the RDFT phase calculations.

The complex-valued periodic signal can be presented as the discrete-time Fourier series:

$$x[k] = \sum_{m=0}^{N-1}|X_m|e^{j\left(m\frac{2\pi kT_w}{NT_1}+\phi_m\right)}. \tag{7}$$

The complex amplitude of the fundamental component at time $k-k_0$ can be calculated from the following formula:

$$X_1[k-k_0] = \\ = \frac{1}{N}\sum_{n=k-k_0-N+1}^{k-k_0}\sum_{m=0}^{N-1}|X_m|e^{j\left(m\frac{2\pi nT_w}{NT_1}+\phi_m\right)}e^{-j\frac{2\pi n}{N}}. \tag{8}$$

After transformations, $X_1[k-k_0]$ is given by:

$$X_1[k-k_0] = \sum_{m=0}^{N-1}|X_m|\frac{1}{N}\frac{\sin\left(\pi\left(m\frac{T_w}{T_1}-1\right)\right)}{\sin\left(\frac{\pi}{N}\left(m\frac{T_w}{T_1}-1\right)\right)}\cdot \\ \cdot e^{j\left(\phi_m+k\frac{2\pi}{N}\left(m\frac{T_w}{T_1}-1\right)-\pi\frac{N-1}{N}\left(m\frac{T_w}{T_1}-1\right)-k_0\frac{2\pi}{N}\left(m\frac{T_w}{T_1}-1\right)\right)}. \tag{9}$$

If the signal period differs from the time window, the complex amplitude of the fundamental component being estimated additionally contains the rescaled amplitudes of all other harmonics. However, within the range of small deviations from the nominal frequency, they do not have a large influence on the amplitude of the fundamental component, and their effect on the phase is negligible. After omitting higher harmonics in (9), the difference between the actual and delayed phase can be expressed as:

$$\varphi_1[k] - \varphi_1[k-k_0] = k_0\frac{2\pi}{N}\left(\frac{T_w}{T_1}-1\right). \tag{10}$$

In order to calculate the phase error expressed by an argument of (6), it is enough to figure out half of the difference between the actual DFT phase and that delayed by N–1. Finally, instantaneous phase of the signal x_1 is estimated based on the following formula:

$$\theta_1[k] = \frac{2\pi k}{N} + 1.5\varphi_1[k] - 0.5\varphi_1[k-N+1]. \tag{11}$$

3.2. Multiple reference frame current controller. A block diagram of the current harmonic controller is shown in Fig. 2. The current control system is composed of the DC component controller, which uses the S-APF phase currents (i_{Fabc}), and the harmonic current controller, which processes harmonic content of the supply currents (i_{Sabc}). The S-APF voltage reference (u_{Fabc}) is the sum of both controller outputs and is accomplished by a pulse width modulator. The harmonic current controller is complemented by an anti-windup scheme, adopted from [9], where it was used for proportional-resonant controllers. The integral anti-windup is useful mainly at low loads (below 50 percent of the nominal load), when the output voltage reference periodically exceeds the limiting value and can lead to instability of the system.

The reactor L_F is modeled as a series RL load, and the transformer Tr is represented by its classical circuit model. The supply voltages and load currents are treated as disturbances to the system. The 18-pulse rectifier creates current harmonics of orders $m = -17, 19, -35, 37, \ldots$ in the stationary $\alpha\beta$ reference frame. The dominant harmonics of the supply voltage usually have orders of $m = -1, 3, -5, 7, -11, 13, \ldots$, where the first of these harmonics corresponds to the asymmetry of the fundamental component. In the dq, m coordinate systems, rotating synchronously with angular frequencies of the dominant harmonics, they become DC quantities and can be eliminated by the synchronous frame controller.

The supply currents i_{Sabc} are transformed to the $\alpha\beta$ coordinate system and deprived of the fundamental component. The

DFT/IDFT filter with phase correction is used to estimate the fundamental harmonic. As shown in Fig. 2, the supply current is subtracted from the output of the filter producing the current error.

The harmonic controller in multiple synchronous reference frames makes use of complex-coefficient PI controllers with cross-coupling decoupling [10, 11].

$$H_{\mathrm{PI}m} = K_{pm} + \left(K_{im} + jm\omega_1 K_{pm}\right)\frac{1}{s} \tag{12}$$

In order to cancel the plant poles by controller zeros, the time constants of the regulator and the filter should be equal, that is $K_{pm}/K_{im} = L/R$, where L and R are the equivalent inductance and resistance of the reactor and the transformer, respectively. Knowing the parameters of the controlled system, the proportional K_{pm} gain can be chosen to achieve the required close-loop bandwidth at harmonic frequency $m\omega_1$.

Unlike in [10], the current controllers in formula (12) have been implemented in MRFs, and not as Vector Proportional-Integral (VPI) controllers in the stationary frame. This is because the MRFs controllers have an inherent ability to adapt to supply frequency and to be flexible in compensating positive and negative harmonic components. If frequency adaptation of VPI controllers is implemented, its computational complexity is comparable to the MRF solution.

In order to simplify the structure of the MRF controller, its proportional part is common for all reference frame controllers and affects the current error $(e_{S\alpha\beta})$ in a direct manner. Consequently, in the dq, m reference frames only the integral and decoupling terms are implemented. The proportional gain $K_{p\alpha\beta}$ is calculated as the sum of all K_{pm} values used in the decoupling terms of the MRF controllers. The outputs of all synchronous controllers are transformed to the stationary reference frame and summed up.

After inverse Clarke transformation, the output voltage reference in each phase is limited, to prevent uncontrolled over-modulation. The DC output voltage is the maximum value that can be generated by VSI. The difference between the actual reference signals of phase voltages and the saturated outputs of the limiting block is fed back to the input of the integral part of the controller. Reference [9] suggests setting the feedback gain K_{AW} between 1 and 10, which has been confirmed in experiments.

Because of the lack of VSI symmetry during the generation of phase voltages, undesirable DC components, which were not present in the grid currents, could arise in the VSI phase currents due to the transformer operation. In order to suppress DC offsets in the VSI phase currents, an additional integration controller with low bandwidth and zero reference value was used.

4. Experimental results

The control algorithm of the S-APF has been verified by means of laboratory tests. Their main goal was to assess the quality of grid currents in steady-state conditions. The task of the current controller is to suppress the dominant harmonics of the following orders: -1; ± 3; $\pm(6n\pm 1)$, with $n = 1, 2, \ldots, 6$. The system and controller parameters are provided in Table 1.

Table 1
Parameters of the proposed AC/DC supply system

E_{S}	Phase to neutral voltage of the supply (50 Hz)	230 V
N	Turns-ratio of series injection transformer	12
C_{L}	Rectifier output capacitance	10 mF
L_{F}	Inductance of switching ripple filter	2.2 mH
R_{F}	Resistance of switching ripple filter	0.06 Ω
L_{Tr}	Equivalent leakage inductance of transformer	3.4 mH
R_{Tr}	Equivalent resistance of transformer	2.94 Ω
f_{s}	Sampling frequency	20 kHz
$\mathrm{K_p}$	Proportional gain for P controller	0.103
K_{pm}	Proportional gain for I controllers in MRFs	0.038
K_{im}	Integral gain for PI controllers	2
$\mathrm{K_{AW}}$	Anti-windup gain	1

The investigations were carried out for the following three cases, marked by notations in parentheses: (Rect.) autonomous operation of the 18-pulse rectifier of apparent power $S_{\mathrm{REC}} = 15$ kVA without an additional grid reactor (Fig. 3); (Rect. + Lf) autonomous operation of the rectifier with a grid reactor (Fig. 4); (Rect. + S-APF) operation of the rectifier with a series active power filter and without an additional reactor (Fig. 5). The presented results of experimental tests have been recorded for three different loads at rectifier output.

The quality of compensation was evaluated based on selected parameters of grid signals measured by the three-phase power quality analyzer Fluke 435. The phase currents (i_S) and voltages (u_S) at the input of the system were measured and registered. In each of Figs. 3–5, the recorded waveforms of grid currents and their spectra are shown for two load conditions. Table 2 summarizes selected measurements of the 18-pulse rectifier supply system for three configurations and load conditions.

Table 2
Selected measurement results of the proposed AC/DC supply system

System	P (kW)	THD_i (%)	PF	I_{neg} (%)	U_{dc} (V)
Rect.	2.18	51.0	0.88	3.1	488
Rect.	7.50	41.6	0.91	4.8	470
Rect.	15.03	22.4	0.97	3,1	455
Rect. + Lf	2.17	24.6	0.94	4.2	483
Rect. + Lf	7.49	8.0	0.98	0.7	460
Rect. + Lf	14.82	4.4	0.98	0.6	441
Rect. + S-APF	2.19	9.6	0.98	1.8	483
Rect. + S-APF	7.43	2.3	1.0	0.4	467
Rect. + S-APF	14.73	0.9	1.0	0.0	452

Subsequent columns of the table contain: active power (P), total harmonic distortion (THD_i) of the supply current in the selected phase, the power factor (PF), current (I_{neg}) unbalance, and the RMS value of the DC voltage (U_{dc}) at rectifier output.

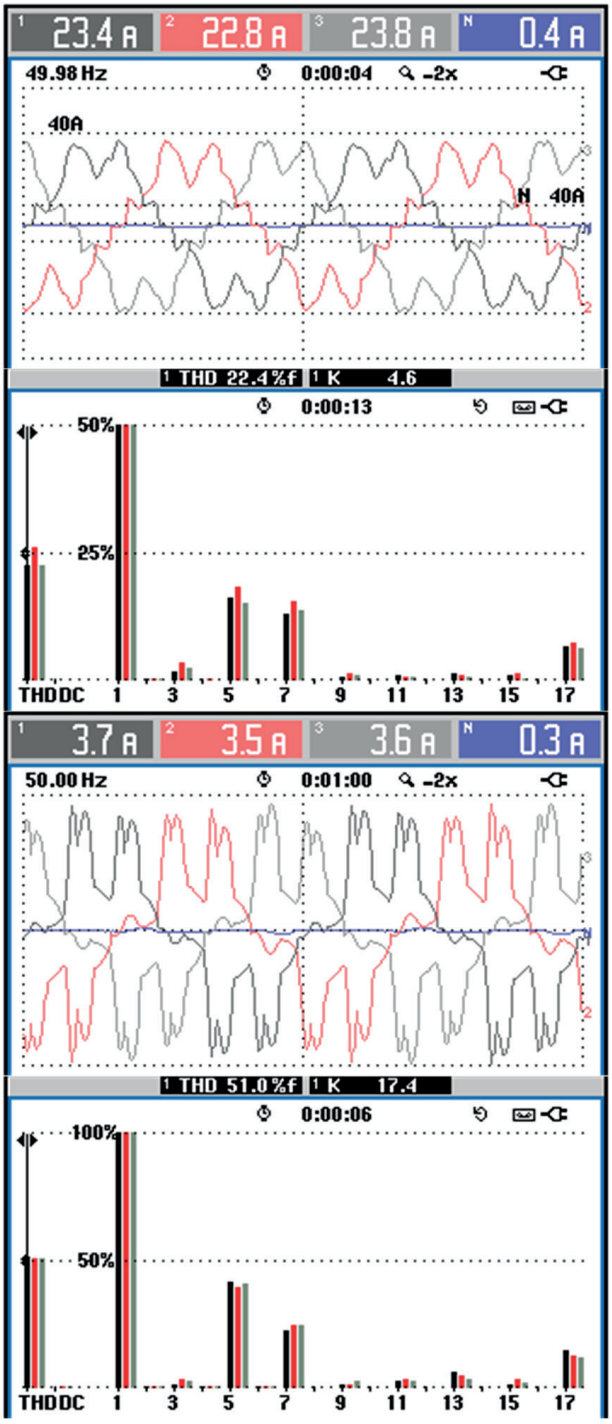

Fig. 3. Oscilograms and spectra of supply current $i_{Sa,b,c}$ in the system without reactor L_F and S-APF at nominal load (upper) and 15% of nominal load (lower)

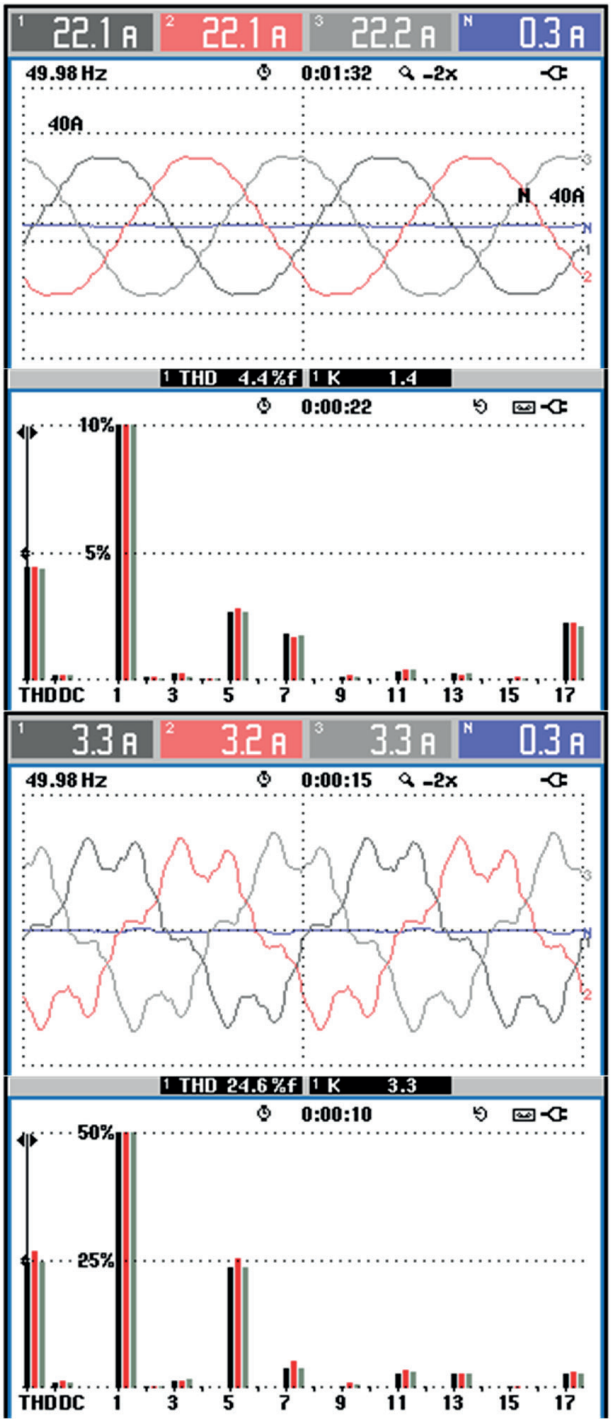

Fig. 4. Oscilograms and spectra of supply current $i_{Sa,b,c}$ in the system with reactor L_F and without S-APF at nominal load (upper) and 15% of nominal load (lower)

As might be expected, the highest current harmonic distortion and unbalance are observed in the case of stand-alone operation of the rectifier without reactor L_R. The additional inductor significantly reduces the current THD level and unbalance percentage. Unfortunately, the output voltage of the rectifier is at the lowest level. For the nominal load, it is equal to approximately 97% of the autonomous operation value.

During operation of the rectifier with the S-APF, the supply current THD is significantly lower than that for the case with an additional reactor. For this configuration of the converter, the current THD also increases with decreasing rectifier load, but even for 15% of the nominal load it is at an acceptably low level.

Overall, the values of all presented power quality indicators are the best for the integrated system.

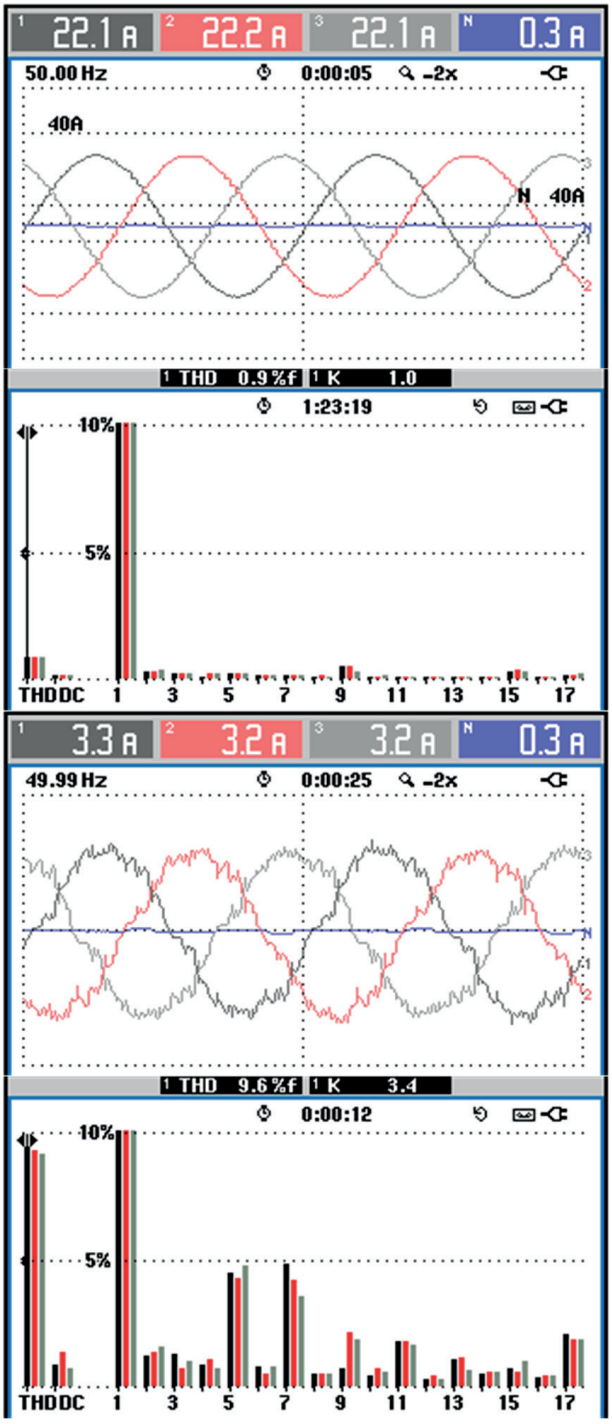

Fig. 5. Oscilograms and spectra of supply current $i_{Sa,b,c}$ in the system without reactor L_F and with S-APF at nominal load (upper) and 15% of nominal load (lower)

5. Conclusions

The paper presents the current harmonic controller for the AC/DC power conversion system based on the 18-pulse diode rectifier with coupled reactors and serial active power filter.

Selective suppression of current harmonics is achieved by using PI controllers with cross-coupling decoupling in multiple reference frames. Thanks to the anti-windup algorithm, during the S-APF output voltage saturation the current harmonics are effectively maintained at levels resulting from the converter's capabilities. To improve grid synchronization of the inverter, a DFT-based algorithm with phase offset correction was implemented.

The proposed current controller has successfully suppressed the dominant harmonic of up to 1850 Hz, and reduced the THD at nominal load from 22% to less than 1%. Along with reduction of the supply current THD, operation of the proposed controller results in the symmetrization of currents and improvement of the power factor.

Acknowledgements. The research presented herein has been funded by the National Centre for Research and Development.

References

[1] B. Singh, S. Gairola, B.N. Singh, A. Chandra, and K. Al-Haddad, "Multipulse AC–DC converters for improving power quality: a review", *IEEE Trans. Power Electron.* 23 (1), 260–281 (2008).

[2] P. Mysiak and R. Strzelecki, "A robust 18-pulse diode rectifier with coupled reactors", *Bull. Pol. Ac.: Tech*. 59 (4), 541–550 (2011).

[3] M. Maciazek and M. Pasko, "Optimum allocation of active power filters in large supply systems", *Bull. Pol. Ac.: Tech*. 64 (1), 37–44 (2016).

[4] H. Fujita and H. Akagi, "An approach to harmonic current-free AC/DC power conversion for large industrial loads: the integration of a series active filter with a double-series diode rectifier", *IEEE Trans. Ind. Appl.* 33 (5), 1233–1240 (1997).

[5] S. Srianthumrong, H. Fujita, and H. Akagi, "Stability analysis of a series active filter integrated with a double-series diode rectifier", *IEEE Trans. Power Electron.* 17 (1), 117–124 (2002).

[6] A.D. Le Roux, H. Mouton, and H. Akagi, "DFT-based repetitive control of a series active filter integrated with a 12-pulse diode rectifier", *IEEE Trans. Power Electron.* 24 (6), 1515–1521 (2009).

[7] P. Mysiak, W. Sleszynski, and A. Cichowski, "Experimental test results of the 150kVA 18-pulse diode rectifier with series active power filter", *International Conference on Compatibility, Power Electronics and Power Engineering (CPE-POWERENG)* (2016).

[8] B.P. McGrath, D.G. Holmes, and J.J.H. Galloway, "Power converter line synchronization using a discrete Fourier transform (DFT) based on a variable sample rate", *IEEE Trans. Power Electron.* 20 (4), 877–884 (2005).

[9] S.A. Richter and R.W.D. Doncker, "Digital proportional-resonant (PR) control with anti-windup applied to a voltage-source inverter", *European Conference on Power Electronics and Applications (EPE)* (2011).

[10] C. Lascu, L. Asiminoaei, I. Boldea, and F. Blaabjerg, "High performance current controller for selective harmonic compensation in active power filters", *IEEE Trans. Power Electron.* 22 (5), 1826–1835 (2007).

[11] C. Lascu, L. Asiminoaei, I. Boldea, and F. Blaabjerg, "Frequency response analysis of current controllers for selective harmonic compensation in active power filters", *IEEE Trans. Ind. Electron.* 56 (2), 337–347 (2009).